Supplementary Information

Epitaxial Growth of Phase-pure and Stable β-Fe_2O_3 Films by Pulsed Laser Deposition Method

Hang Yin,[a,b] Chenwei Ni,[a,b] Jiangshan Qu,[a] Pengfei Zhang,[a,b] Xuefei Zhao,[a,b] Jingying Shi,*[,a,c] and Can Li *[,a]

[a.] *State Key Laboratory of Catalysis, Dalian National Laboratory for Clean Energy, Dalian Institute of Chemical Physics, Chinese Academy of Sciences, Dalian 116023, China. E-mail: canli@dicp.ac.cn; jingyingshi@dicp.ac.cn*
[b.] *University of Chinese Academy of Sciences, Beijing 100049, China.*
[c.] *Center of Materials Science and Optoelectronics Engineering, University of Chinese Academy of Sciences, Beijing 100049, China.*

Growth of ITO films on YSZ substrate

The ITO film located between the YSZ substrate and β-Fe_2O_3 serves not only as an 'induction layer' for the epitaxial growth of β-Fe_2O_3 but also as a conductive layer for encapsulating β-Fe_2O_3 as an electrode for electrochemical testing. Therefore, optimizing the resistance and charge mobility of the ITO film is essential, with the specific optimization parameters outlined in Table S1.

ITO films were deposited on the (100) and (111) YSZ substrates, which are provide a similar cubic lattice structure for epitaxial growth. A YSZ substrate of 5×5 mm was adhered to a metal holder using SPI conductive silver paste. After drying on a heating stage, the substrate was put into the PLD chamber. The chamber was pumped to a vacuum of 1×10^{-6} Torr using a mechanical pump and a molecular pump before heating commenced. Once the substrate reached the target temperature, oxygen was introduced into the chamber, and then it comes with sputtering of the target material. During the sputtering process, the target was rotated while simultaneously rounded with raster.

The resistivity and carrier mobility of ITO films on (100) YSZ substrate deposited under different conditions (Table S1) were measured using the four-probe method. Conductive silver paste was applied at the four corners of the ITO films with size of 5 × 5 mm, onto which four probe electrodes were pressed. The test results are presented in the Figure S1, considering the requirement for the ITO films to exhibit both low resistivity and high carrier mobility, the growth conditions of Sample 1 were selected as the optimal conditions for subsequent ITO film deposition.

Therefore, we deposited ITO films on (100) and (111) YSZ substrate under oxygen pressure of 10 mTorr, deposition temperature of 875℃. According to the XRD results of the ITO/YSZ are shown in Figure S2(a), only diffraction peaks of (222), (444) planes of ITO can be observed for the ITO film grown on (111) YSZ substrate; only diffraction peaks of (400), (600) and (800) planes of ITO can be observed for the ITO film grown on (100) YSZ substrate. These results indicate that the ITO films were epitaxial grown along with the [100] and [111] axis of YSZ substrates, respectively. The roughness of the ITO films on (100) YSZ substrate is 1.31 nm, whereas the is 0.65 nm for the ITO films on (111) YSZ substrate, which are both smooth thin films (Figure S2b and c).

	Laser fluence/ mJ cm^{-2}	Oxygen pressure/ mTorr	Deposition temperature/ ° C	Repetition rate/Hz	Laser Shot/ pulses	Cooling rate/dpm
①	0.9	10	875	1	2000	25
②	0.9	10	800	1	2000	25
③	0.9	10	900	1	2000	25
④	0.9	50	875	1	2000	25
⑤	0.9	30	875	1	2000	25

Table S1. The deposition conditions of ITO films grown on (100) YSZ substrate.

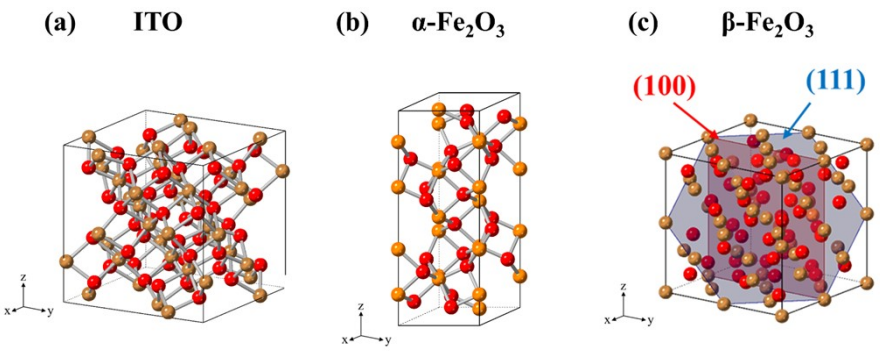

Figure S1. Crystal structures of (a) ITO; (b) α-Fe_2O_3; (c) β-Fe_2O_3. ITO has a cubic crystal structure with cell parameter of 10.12 Å; β-Fe_2O_3 has a cubic crystal structure with cell parameter of 9.4 Å; α-Fe_2O_3 exhibits a rhombohedral structure ($^{a}{}_{\alpha} = {}^{b}{}_{\alpha}$ = 5.03 Å, $^{c}{}_{\alpha}$ = 13.74 Å, γ =120°)

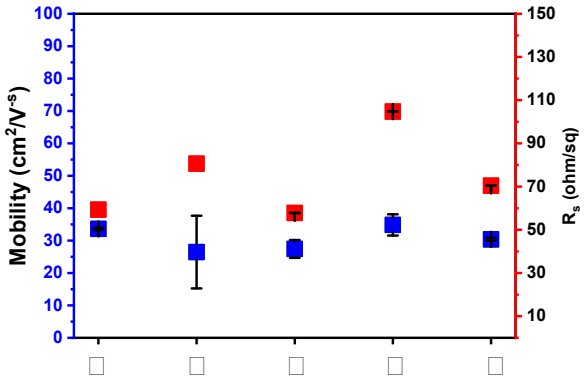

Figure S2. The resistance and mobility of ITO films deposited under different temperature. The measurements were conducted using a four-probe method, with each sample tested three times under identical conditions, and the results averaged. Considering both resistance and carrier mobility, the final optimized oxygen pressure for the ITO film was determined to be 10 mTorr, with a deposition temperature of 875 °C.

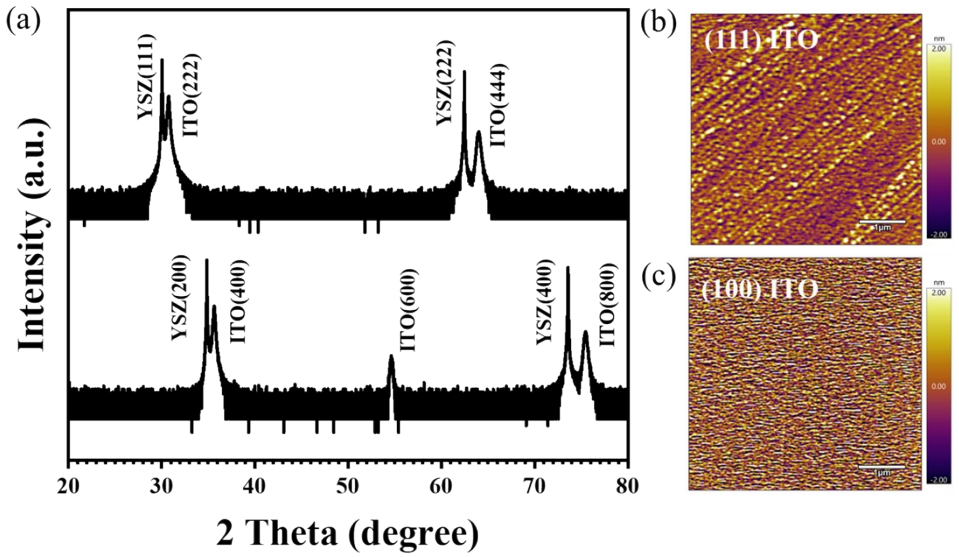

Figure S3. (a) X-ray diffraction characterization of ITO grown on (100) and (111) YSZ. (b) and (c) are the top-view AFM images for (111) ITO/YSZ and (100) ITO/YSZ, respectively.

Table S2. The Hall resistivity, mobility and carrier concentration of ITO films grown on (100) and (111) YSZ were measured using an HL5550 LN2 Cryostat system at room temperature. The thickness of the ITO films is ~80 nm.

	Resistivity ($\Omega \cdot sq^{-1}$)	Hall mobility ($cm^2 \cdot V^{-1} \cdot s^{-1}$)	Carrier concentration (cm^{-2})
(100)ITO/YSZ	35.4	37.0	-4.7e+15
(111)ITO/YSZ	39.7	32.4	-4.8e+15

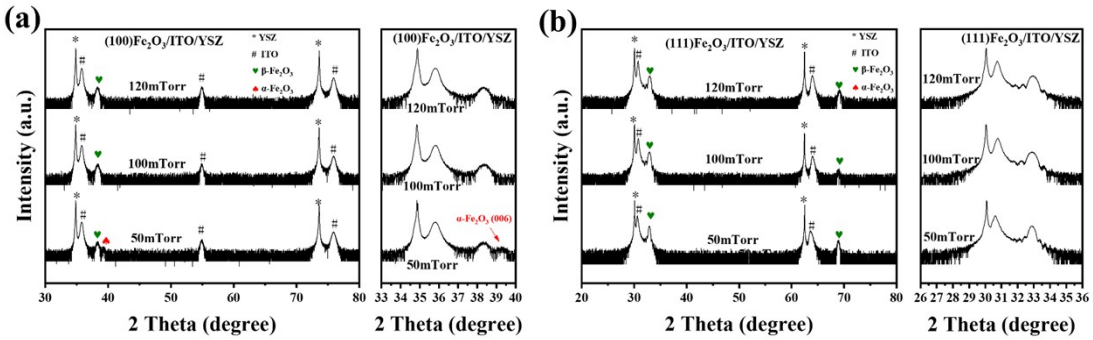

Figure S4. XRD patterns of (a) (100) β-Fe_2O_3/ITO/YSZ and magnified peaks of (400) of β-Fe_2O_3; (b) (111) β-Fe_2O_3/ITO/YSZ and magnified peaks of (222) of β-Fe_2O_3. β-Fe_2O_3 films were deposited under oxygen pressure of 50-120 mTorr. Pure β-Fe_2O_3 films can be obtained under oxygen pressure higher than 100 mTorr for (100) β-Fe_2O_3/ITO/YSZ, and the lower oxygen pressure leading to greater thickness of films for (111) β-Fe_2O_3/ITO/YSZ.

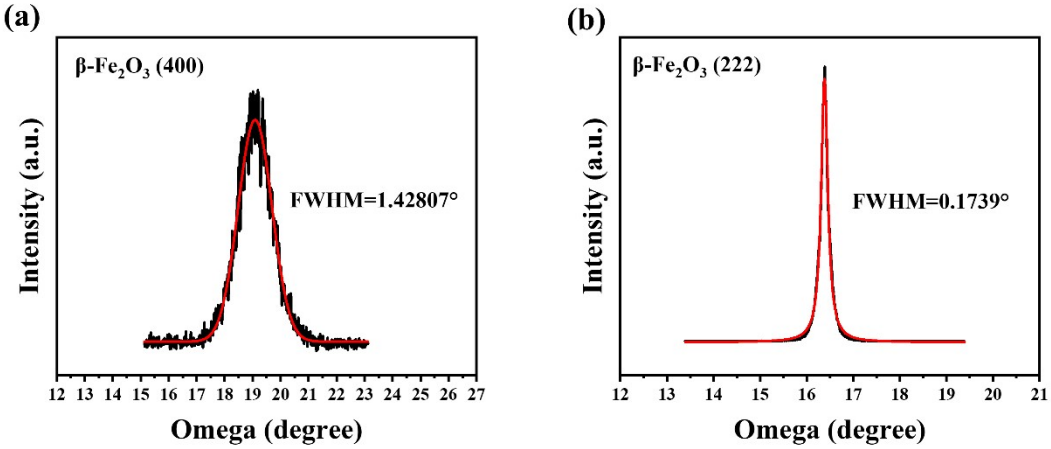

Figure S5. Rocking curves of (a) peak of (400) plane for (100)β-Fe_2O_3 film; (b) peak of (222) plane for (111)β-Fe_2O_3 film. The rocking curves (ω scan) were performed using an automated multipurpose X-ray diffractometer SmartLab 9kW with a multi-dimensional pixel array detector HyPix-3000 equipped with a Ge(220)×2 monochromator. As the sample is rotated about omega axis, the detector is rotated at twice the rate so that 2Theta=2·Omega, producing a coupled omega-2theta scan.

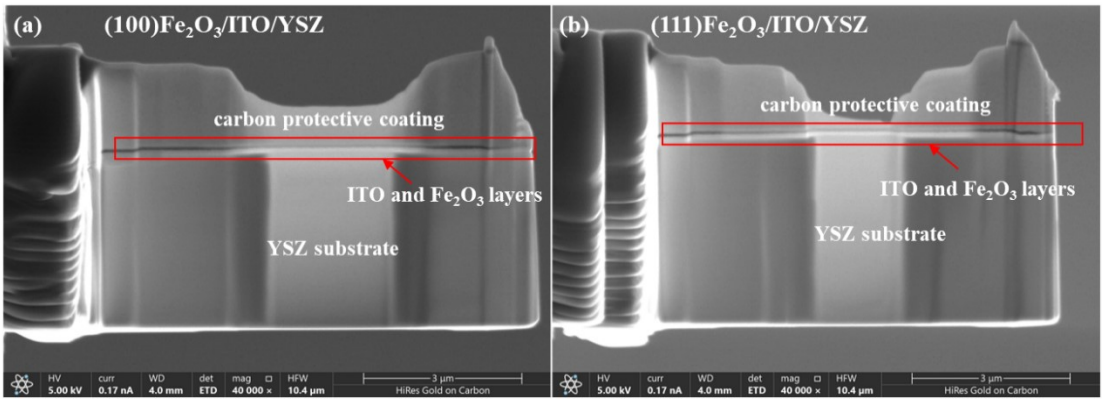

Figure S6 SEM images of the films after milling by focused ion beam (FIB). (a) (100) β-Fe_2O_3/ITO/YSZ; (b) (111) β-Fe_2O_3/ITO/YSZ.

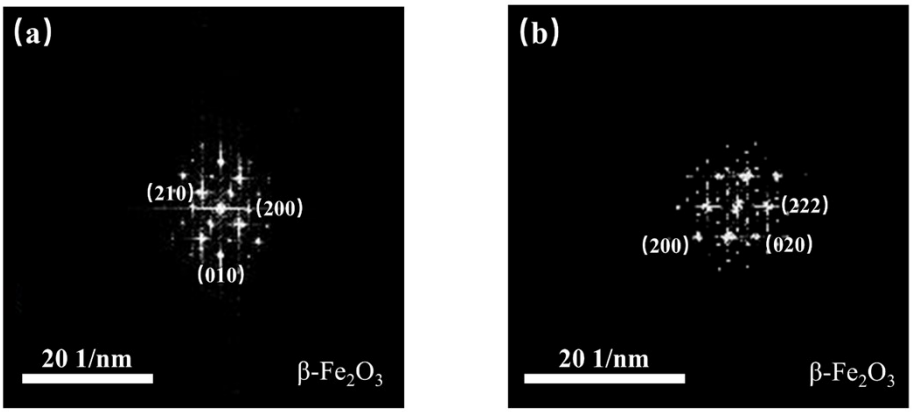

Figure S7. SAED images of (a) (100) β-Fe_2O_3 and (b) (111)β-Fe_2O_3. In Figure S7a, the shortest interplanar spacings between the diffraction and the center transmission spots are approximately 4.14, and 8.1 Å, which correspond well to those for β-Fe_2O_3(200), and (010) planes, respectively. In Figure S7b, the shortest interplanar spacings between the diffraction and the center transmission spots are approximately 4.56, and 2.72 Å, which agree well with those of β-Fe_2O_3(200), and (222) planes, respectively.

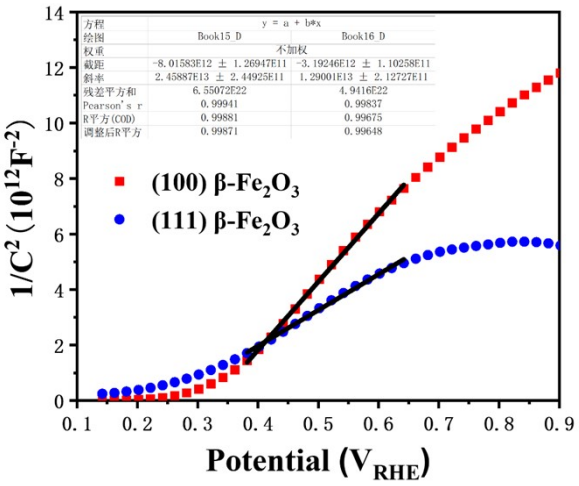

Figure S8. Mott–Schottky plots and fitting results for the β-Fe_2O_3 thin films.

For Mott-Schottky,

$$\frac{1}{C^2} = \frac{2}{\varepsilon\varepsilon_0 A^2 e N_D}(V - V_{fb} - \frac{k_B T}{e})$$

A plot of $1/C^2$ against V should yield a straight line from which V_{fb} can be determined from the intercept on the V axis. Therefore, value of carrier concentration N_D can be found from the slope knowing ε and A:

$$slope = \frac{2}{\varepsilon\varepsilon_0 A^2 e N_D}$$

Here, ε is the relative dielectric constant and ε = 10; ε_0 is the dielectric constant of vacuum and ε_0 = 8.85 × 10^{-12} F/m, e is the electronic charge and e = 1.6 × 10^{-19} C, the electrode area is 0.25 cm^2. So the calculated carrier concentration (electron density) is 8.06 × 10^{18} cm^{-3} for (100)β-Fe_2O_3, and 4.41 × 10^{18} cm^{-3} for (111)β-Fe_2O_3.

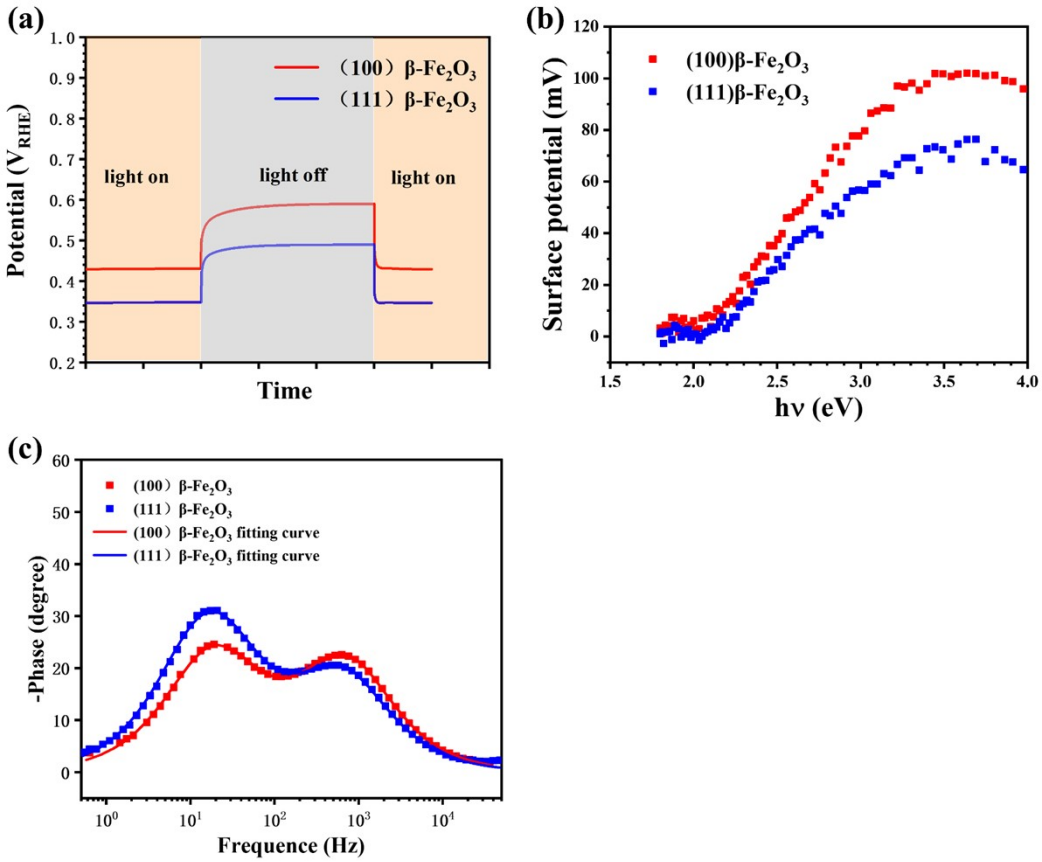

Figure S9. (a) Open circuit voltage (OCP) of (100) β-Fe_2O_3 and (111) β-Fe_2O_3 under dark and irradiation conditions; (b) Surface photovoltage spectra of (100) β-Fe_2O_3 and (111) β-Fe_2O_3; (c) Bode plots of (100) β-Fe_2O_3 and (111) β-Fe_2O_3.

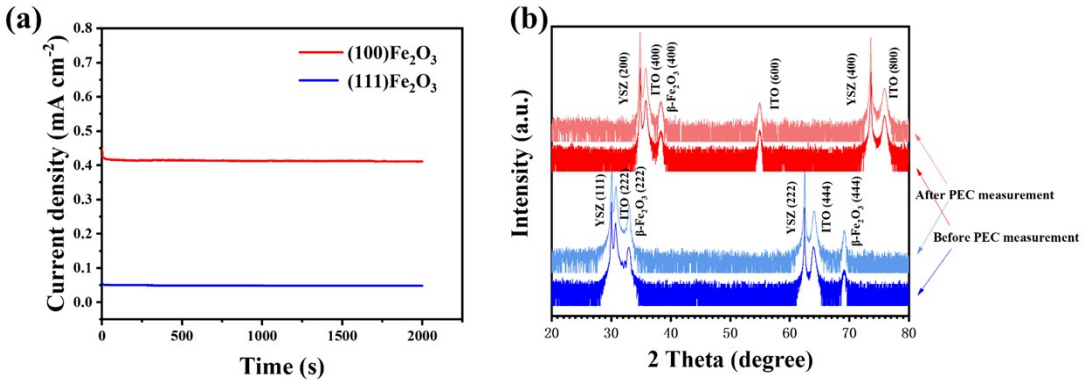

Figure S10. (a) I-t curves of (100) β-Fe_2O_3 and (111) β-Fe_2O_3 at 1.5 V_{RHE} under AM 1.5G simulated sunlight; (b) XRD patterns of (100) β-Fe_2O_3 and (111) β-Fe_2O_3 before and after PEC measurement.